Springer

Journal of Mechanical Science and Technology 22 (2008) 2056~2061

Journal of
Mechanical
Science and
Technology

www.springerlink.com/content/1738-494x
DOI 10.1007/s12206-008-0709-x

An estimation of failure stress condition in rocker arm shaft through FEA and microscopic fractography †

Dong Woo Lee[1], Seok Swoo Cho[2] and Won Sik Joo[1,*]

[1]*Department of Mechanical Engineering, Dong-A University, 840, Hadan2-dong, Saha-gu, Busan 604-714, Korea*
[2]*Department of Vehicle Engineering, Kangwon National University, 253, Gyo-dong, Samcheok-si, Gangwon-do 245-711, Korea*

(Manuscript Received March 11, 2008; Revised June 29, 2008; Accepted July 15, 2008)

Abstract

The failure analysis of a rocker arm shaft for a 4-cylinder SOHC engine is presented. Fracture accidents occur in the interface between the rocker arm shaft and the engine block. These fractures are responsible for bolt tightening. The failure boundary condition is estimated by using an orthogonal array and ANOVA. Stress range is obtained by fatigue striation spacing and fracture mechanical simplification. Minimum and maximum stresses are predicted by FEA for the failure boundary condition. This study shows that the stress conditions for a fracture surface with fatigue striation can be determined by FEA and SEM.

Keywords: Orthogonal array; ANOVA; Fractography; Fatigue striation; SEM; FEA; Stress intensity factor

1. Introduction

Machine parts subjected to fluctuating or cyclic loads experience repeated stresses. In such a case, fatigue failure sometimes occurs. More than 80% of failure accidents are due to fatigue resulting from incorrect designs of machine parts. Failure analysis provides valuable information on similar failure accidents that may be useful for improving existing designs or developing new products [1, 2].

The rocker arm shaft that supports the intake and exhaust valves of an engine passes through the center of the rocker arm. The results from a questionnaire on the trouble parts of vehicles revealed that the failure of the rocker arm shaft accounted for 30% of engine faults and became the main cause of fatal traffic accidents. Only design modifications based on failure analysis can prevent these accidents.

Usually, the failure analysis of broken parts consists of quantitative and qualitative methods. Qualitative methods include the use of the naked eye, metallurgical microscope, etc. Quantitative methods use SEM (Scanning electron microscope), X-ray diffraction, etc. Among the quantitative methods, SEM can estimate the stress amplitude of fatigue failure parts by using the relation between striation spacing and the stress intensity factor range. When the stress amplitude and stress ratio are obtained at the same time, the applied stress condition can also be easily obtained [2, 3].

Murakami et al. [4] predicted the stress condition applied to the Al 2017-T7 alloy using the relation between striation spacing and striation height.

Cho et al. [5, 6] proposed a failure analysis for the broken parts with no striation pattern like ceramics by using a relation between the stress intensity factor and the plastic zone depth. Their method was applied to contaminated or corroded parts.

The above methods are very useful because they can find the stress conditions for cracked parts. The former case can be applied to failure parts having a known striation height, but the latter case requires

† This paper was recommended for publication in revised form by Associate Editor Youngseog Lee

*Corresponding author. Tel.: +82 51 200 7641, Fax.: +82 51 200 7656
E-mail address: wsjoo@dau.ac.kr

excessive experiment time because of the many experiments that must be performed. Therefore, this study aims to show that the failure stress condition applied to a rocker arm shaft can be predicted by the use of an orthogonal array, SEM and FEA. Experiment time will be shortened considerably because we used striation spacing as a failure analysis parameter.

2. Failure accident of rocker arm shaft

2.1 Structure of rocker arm shaft

Fig. 1 shows an assembly drawing of a rocker arm shaft for a 4-cylinder SOHC engine. The rocker arm shafts are tightened by bolts on the engine block. The rocker arms are installed on the rocker arm shaft for the intake and exhaust valves. Fig. 2 indicates the loads (A, B, C and D) applied to the rocker arm shaft by cam movement.

2.2 Failure accident of rocker arm shaft

A typical fractured rocker arm shaft is shown in Fig. 3(a). The traveling distance of the vehicle used in this study is 115,320 km. The dominant fracture was due to the through hole in the rocker arm shaft. The crack was initiated at the bottom of the through hole and subsequently propagated along its sidewall, as shown in Fig. 3(b). The fracture surface is divided into the fatigue initiation region A, fatigue propagation region B, and the final fracture region C by separate surfaces.

The load applied to the rocker arm shaft by cam movement induced tensile bending stress and hence, initiated and propagated the fatigue crack. But the compressive bending stress by the movement of another cam and the unstable boundary condition caused the separate surfaces to compress each other.

Fig. 4 shows the fracture surface by SEM with typical fatigue striation. This result shows that the failure of the rocker arm shaft was caused by the bending load and unstable boundary condition.

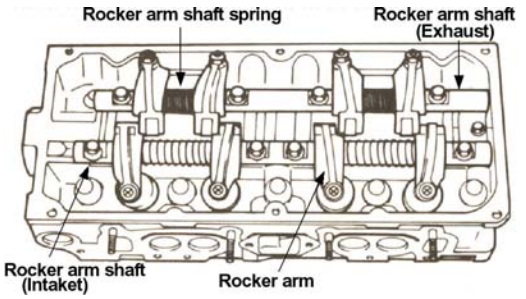

Fig. 1. Assembly drawing of rocker arm shaft.

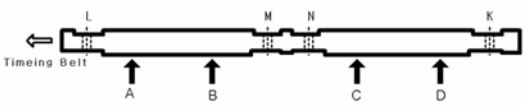

Fig. 2. Load conditions applied to rocker arm shaft.

3. Estimation of failure boundary conditon by orthogonal array

From past experience [7], we found that the failure

(a) Failure of rocker arm shaft in the 4-Cylinder SOHC engine

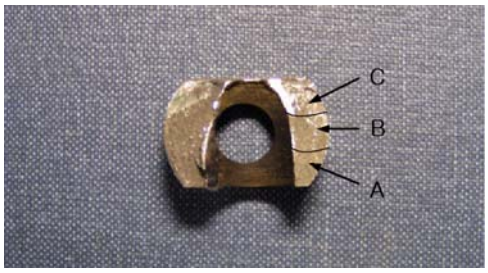

(b) Fractured surface of rocker arm shaft

Fig. 3. Photographs of rocker arm shaft.

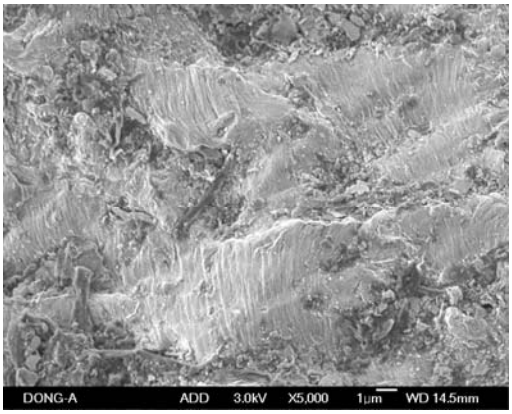

Fig. 4. SEM photographs of fatigue crack growth stage in rocker arm shaft.

Table 1. The most dangerous failure boundary condition of rocker arm shaft.

Load	Level of factor			
	L	M	N	K
A	3	2	1	1
B	3	2	1	1
C	2	2	1	2
D	**3**	**2**	**1**	**3**

Table 2. Tightening condition of rocker arm shaft under actual failure boundary condition.

Load	Level of factor			
	L	M	N	K
D	1	2	1	3
	1	3	1	3

of a rocker arm shaft was mainly due to blot joint conditions. Boundary conditions 1 and 2 represent bolt torques of 19.6 N·m and 0 N·m, respectively. Boundary condition 3 represents a bolt that was loosened by a repeated mechanical load. An orthogonal array of $L_9(3^4)$ was used to determine the boundary conditions of the rocker arm shaft [8]. Responses were obtained by stress measurement experiments. Table 1 shows the failure boundary conditions as determined by ANOVA. Table 2 shows the actual failure boundary conditions.

4. Failure analysis of rocker arm shaft by striation spacing, stress intensity factor, and FEA

Striation spacing is strongly related to fatigue crack propagation rate. Paris' law represents a good relationship between the rate of fatigue crack propagation and the range of the stress intensity factor. The range of the stress intensity factor can be predicted by striation spacing and the rate of fatigue crack propagation. But, failure stress conditions cannot be evaluated by only these parameters. Therefore, this study obtained the stress ratio of the rocker arm shaft by using an orthogonal array, ANOVA and FEM. Failure stress conditions were obtained by using the relation between stress intensity factor range and stress ratio in the fracture mechanical simplification of failure parts.

4.1 Fracture surface analysis by SEM

When a machine part is fractured, this failure should be examined clearly to prevent a recurrence of the same failure accident. The failure loading condition of fractured parts is acquired by SEM or X-ray fractography. X-ray fractography, however, is unsuitable for failure analysis because it requires a long experiment time. If a pollutant, the second damage, and no striation pattern appear on the fracture surface, it is difficult to use a scanning electron microscope in the failure analysis. But, if the failure surface shows striation, failure loading condition can be predicted most simply by using SEM. Fig. 4 shows region B in Fig. 3(b) by SEM. In Fig. 4, the striation spacing on the fracture surface of the rocker arm shaft is 2.5×10^{-4} mm.

Table 3. Material properties of rocker arm shaft.

Tensile Strength, σ_t (MPa)	769
Yield Strength, σ_{ys} (MPa)	710
Young's modulus, E(GPa)	205
Poisson's ratio, ν	0.29
Elongation (%)	6.27

4.2 Quantitative failure analysis of rocker arm shaft

4.2.1 Relationship between striation spacing and stress intensity factor range

Fracture Eq. (1) is derived from the relation between striation spacing (S_t) and crack propagation rate (da/dN) and the relation between crack propagation rate (da/dN) and the stress intensity factor range (ΔK) [9].

$$S_t = 9.4(1-\nu^2)(\Delta K^2 / E) \quad (1)$$

where ν and ΔK represent Poisson's ratio and the range of the stress intensity factor , respectively.

Table 3 shows the material properties of the rocker arm shaft. The material property tests were carried out by using the electro–mechanical test system with 98 kN capacity (INSTRON model 1337). Substituting numerical values for the parameters (Poisson's ratio, Young's modulus, and striation spacing) into Eq. (1), the stress intensity factor range of the rocker arm shaft was found to be ΔK =34.93 $MPa\sqrt{m}$.

4.2.2 Relationship between stress intensity factor range and stress range

Fatigue striations, which correspond numerically to the number of loading cycles, appear in fatigue crack propagation stage 2. The sub-committee on fractography in JSME has indicated a good correlation between striation spacing and fatigue crack growth rate

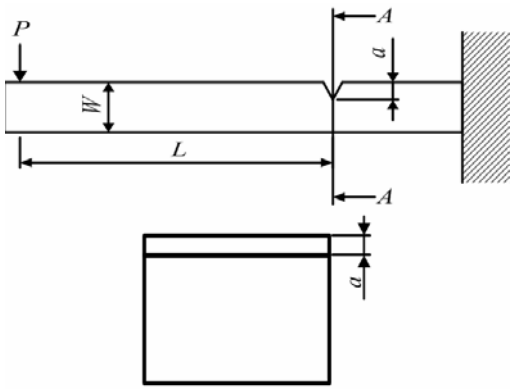

Fig. 5. Stress intensity factor under bending loads.

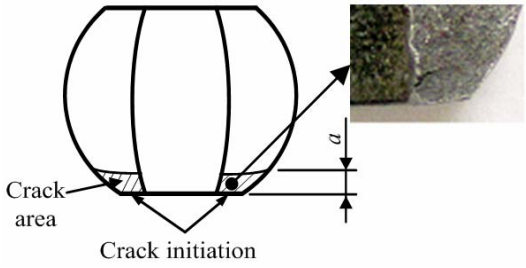

Fig. 6. Fractured section of rocker arm shaft.

in the region of $10^{-4} \sim 10^{-3}$ mm/cycle [3].

Fig. 5 shows the rocker arm shaft idealized as a beam with a rectangular cross section. The stress intensity factor range ΔK is given by bending stress range $\Delta\sigma_B$ and crack length a [10].

$$\Delta K_I = \Delta\sigma_B \sqrt{\pi a} \cdot F_I(a/W) \tag{2}$$

$$F_I = 1.122 - 1.40(a/W) + 7.33(a/W)^2 - 13.08(a/W)^3 + 14.0(a/W)^4 \tag{3}$$

Where $\Delta\sigma_B$, a and W represent the bending stress range, crack length and specimen width, respectively.

The failure location of the rocker arm shaft is shown in Fig. 6. The through hole of the rocker arm shaft was examined and it was found that the failure was due to a loosening of the bolt. Crack length and width measured at the crack initiation region were 0.001 m and 0.013 m, respectively. We predicted the stress range $\Delta\sigma$ =592.42 MPa by substituting the stress intensity range, crack length, and width of the rocker arm shaft into Eq. (2).

The formation of striations is sensitive to the stress ratio as well as the stress intensity factor range. Therefore, minimum and maximum stresses applied to a rocker arm shaft cannot be estimated by using only the striation spacing. Actual failure stress condition can be obtained by using the relationship between the range of the stress intensity factor and the striation spacing, given the stress ratio.

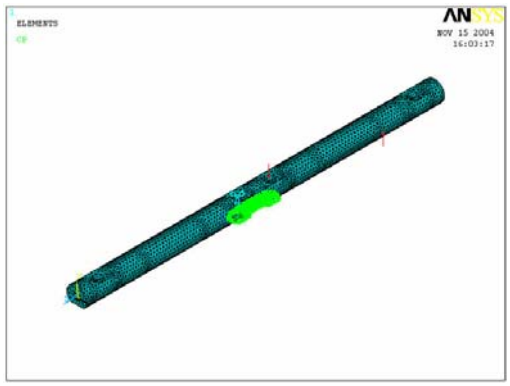

Fig. 7. Loading and boundary conditions of rocker arm shaft.

4.2.3 FE analysis of rocker arm shaft

FEA on the failure boundary condition determined by an orthogonal array and ANOVA were performed. Fig. 7 shows the finite element model for the rocker arm shaft. Finite element modeling was performed by using the commercial FEA software ANSYS Ver 7.0. Most of the significant geometric features were modeled, and a relatively finer mesh was used for the region of failure than for other regions. The finite element used in this study was a 3D 10-node tetrahedral structural solid element with three degrees of freedom at each node. The number of finite elements and nodes was 42754 and 25203, respectively. The global mesh density was chosen to minimize the discretization errors in the failure region. Material property data considered for the numerical simulation are summarized in Table 3. The boundary condition for the tightened bolt indicated a fixed y-direction displacement in the interface between the engine block and the rocker arm shaft and a full load in the interface between the bolt and the rocker arm shaft. The boundary condition before the perfect loosening of the bolt indicated a fixed y-direction displacement in the interface between the engine block and the rocker arm shaft, and all the degrees of freedom were fixed in the interface between the bolt and the rocker arm shaft. The boundary condition after the perfect loosening of the bolt meant that all the degrees of freedom were free in the interface between the engine block and the rocker arm shaft and in the interface between

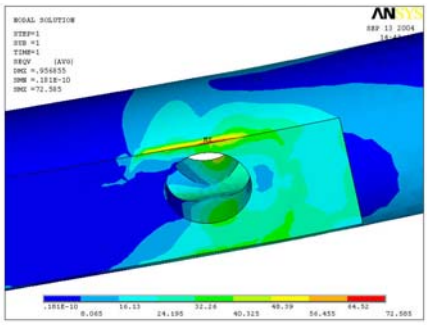

(a) $\sigma_{max} = 711MPa$

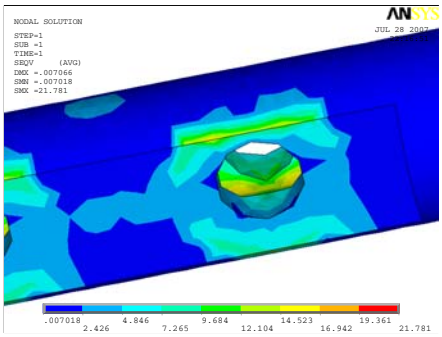

(b) $\sigma_{min} = 161MPa$

Fig. 8. FEA results of rocker arm shaft.

the bolt and the rocker arm shaft.

The load applied to the rocker arm shaft was classified as bolt clamping force and cam stroke force. A cam stroke force was applied to the rocker arm by cam rotation and the force was 549 N. In the FEA, the cam stroke force was applied to the interface between the rocker arm and the rocker arm shaft and was assumed as a partial distribution pressure.

Fig. 8(a) shows the FEA result for the failure boundary condition obtained from orthogonal array and ANOVA. In this figure, the maximum stress is 711MPa. Fig. 8(b) shows the FEA result for the rocker arm shaft subjected to only the clamping force. In this figure, the minimum stress is 161MPa. Therefore, the stress range $\Delta\sigma$ at the failure region was 711 MPa -161MPa = 550MPa.

Fig. 9 compares the stress range from fracture mechanics with the stress range from FEA. The failure boundary condition obtained from orthogonal array and ANOVA was valid because the relative error between the test results obtained from failure analysis of rocker arm shaft and FEA results was within 7%. Therefore, the maximum and minimum stresses applied to the rocker arm shaft were 711 MPa and 161 MPa, respectively.

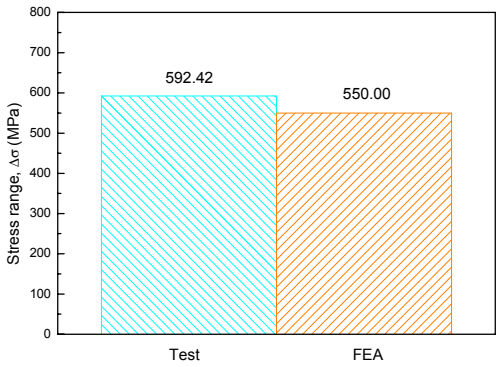

Fig. 9. Comparison between test and FEA results in stress range.

5. Conclusions

This study estimated the failure stress condition of a rocker arm shaft by using striation spacing and FEA and the results were as follows.

(1) FEA results for the failure boundary condition obtained from orthogonal array indicated that the maximum and minimum stresses were 711 MPa and 161 MPa, respectively. The stress range $\Delta\sigma$ was 550 MPa.

(2) The stress range $\Delta\sigma$ obtained from the relationship between striation spacing and the range of the stress intensity factor was 592.42 MPa.

(3) The failure boundary condition estimated by using an orthogonal array and ANOVA was very useful because the relative error between the stress ranges obtained from striation and the stress ranges from FEA fell within 7%.

Acknowledgment

This Paper was Supported by Dong-A University Research Fund.

References

[1] J. A. Collins, *Failure of Materials in Mechanical Design, 2nd ed.,* John Wiley & Sons, New York, (1993) 178.

[2] R. Koterazawa, R. Ebara and S. Nishida, *Current Japanese Material Research-Vol.6 Fractography*, Elsevier Applied Science, (1990) 289-311.

[3] Report of the sub-committee on fractography, *Journal of the Japan Society of Mechanical Engineers*, 76 (1973) 1203.

[4] Y. Murakami, K. Furukawa and N. Shiraishi, Prediction of Service Loading from the Width and Height of Striation of 2017-T4 Al Alloy, *Journal of Society Material Science*, 39 (1990) 1113-1118.

[5] S. S. Cho, D. Y. Jang and W. S. Joo, A Study on Residual Stress for Fatigue Fracture Surface in General Purpose Structural Steel using X-ray Diffraction, *Transactions of the Korean Society of Automotive Engineers*, 7 (1999) 248-261.

[6] S. H. Hong, D. W. Lee, S. S. Cho and W. S. Joo, A Study on the X-Ray Fractography of Turbine Blade under Fatigue Load, *Journal of the Korean Society for Precision Engineering*, 19 (2002) 65-71.

[7] D. W. Lee, S. J. Lee, S. S. Cho and W. S. Joo, Failure of Rocker Arm Shaft for 4-Cylinder SOHC Engine, *Engineering Failure Analysis,* 12 (3) (2005) 405-412.

[8] M. S. Phadke, Quality Engineering Using Robust Design, Prentice Hall, New Jersey, (1989).

[9] K. Matsui, Y. Hirose, A. Chadani and K. Tanaka, Application of X-Ray Fractographic Technique to Actual Failure Analysis, *Journal of Material Science*, 24 (1975) 117-128.

[10] Brown, W. F., Jr. and Strawley, Plane Strain Crack Toughness Testing of High Strength Metallic Materials, J., ASTM STP 410, 1-65, (1966).

Won Sik Joo received his Ph.D. degree from Dong-A University in 2003 and is currently a Visiting Professor for the De-partment of Mechanical Engineering at Dong-A University.